Effect of Measurement Backaction on Adiabatic Coherent Electron Transport

Jérôme Rech[1,2] and Stefan Kehrein[1]

[1]*Physics Department, Arnold Sommerfeld Center for Theoretical Physics and Center for NanoScience, Ludwig-Maximilians-Universität, Theresienstrasse 37, 80333 Munich, Germany*

[2]*Centre de Physique Théorique, UMR 6207, Case 907, Luminy, 13288 Marseille Cedex 9, France*

(Received 21 April 2010; published 31 March 2011)

We study the backaction of a nearby measurement device on electrons undergoing coherent transfer via adiabatic passage (CTAP) in a triple-well system. The measurement is provided by a quantum point contact capacitively coupled to the middle well. We account for this continuous measurement by treating the whole {triple-well + detector} as a closed quantum system. This leads to a set of coupled differential equations for the density matrix of the enlarged system which we solve numerically. This approach allows us to study a single realization of the measurement process while keeping track of the detector output, which is especially relevant for experiments. In particular, we find the emergence of a new peak in the distribution of electrons inside the detector, accompanied by a drop in the fidelity of the protocol.

DOI: 10.1103/PhysRevLett.106.136808 PACS numbers: 73.23.Hk, 03.67.−a, 05.60.Gg, 73.63.Kv

Solid-state based quantum computer architectures are currently the focus of active experimental and fundamental research, as many of them offer the promise of being scalable, therefore opening the way to significant improvements in efficiency of certain algorithms. An essential feature of many proposals for scalable quantum computation is the coherent transport over large distances of quantum information, encoded, e.g., in electron spins.

A recent method of all-electrical population transfer for electrons has been suggested in solid-state systems consisting of a chain of potential wells [1]. Termed coherent transfer by adiabatic passage or CTAP, this technique is a spatial analogue of the STImulated Raman Adiabatic Passage (STIRAP) protocol [2] used in quantum optics to transfer population between two long-lived atomic or molecular energy levels. The CTAP scheme amounts to transporting electrons coherently from one end of the chain to the other by dynamically manipulating the tunnel barriers between potential wells.

There have been several proposals to perform the CTAP scheme in triple-well solid-state systems such as quantum dots [3–6], ionized donors [7] or superconductors [8]. Similarly, this technique has been put forward as a means to transport single atoms [9] and Bose-Einstein condensates [10] within optical potentials. Recently, a classic analogue of CTAP has also been demonstrated experimentally, using photons in a triple-well optical waveguide [11]. The CTAP protocol therefore has both a quantum optics and a condensed matter version, thus raising interest well beyond the field of quantum information.

The implementation of the CTAP protocol naturally brings about the question of its observation. The most striking signature of CTAP is the vanishing occupation of the middle potential well, which can be monitored using a sensitive electrometer. In solid-state devices, this is usually achieved using ballistic quantum point contacts (QPC). The electric current flowing through the QPC is influenced by the presence of an electronic charge in its close environment, thus turning the QPC into a charge detector. One may then wonder to what extent this charge detection is invasive, a matter that is also directly relevant for possible applications for quantum information purposes, as the measurement backaction in the above setup can be related to the influence of a decohering environment along the chain.

Now it is largely believed that the CTAP scheme is relatively robust against this type of measurements precisely because the middle potential well is barely populated. However, recent work [12] concentrating on the decoherence aspects associated with nonlocal measurements suggests otherwise. In this Letter, we study the measurement backaction of the QPC on the CTAP scheme, focusing on the effects of a continuous measurement process. The measurement can take a significant amount of time leading to a continuous evolution of the system and thus posing a nontrivial time-dependent problem, complicated by the dynamic tuning of the tunneling rates between potential wells. Our approach closely follows an alternative derivation of the Bayesian formalism developed by Korotkov [13]. The advantages over the conventional master equation are threefold. First, it allows for the analysis of a particular realization of the measurement process, rather than capturing the behavior of the system averaged over many measurements. Second, it enables us to keep track of the detector output over the duration of the transfer, providing us with information about the time evolution of the system, relevant to upcoming experiments. Third, it provides a microscopic model for the unavoidable decoherence rate due to measurement backaction: In Ref. [1] the fidelity of the CTAP process has been analyzed as a function of some given decoherence rate appearing as an additional parameter, while we will be able to make a direct

connection between which path information and loss of fidelity. This is particularly important from the quantum information point of view, since it shows that any environment providing which path information—even for sites with suppressed occupancies—reduces the fidelity.

We consider a triple-well solid-state system, whose Hamiltonian is characterized by the time-dependent tunneling rate $\Omega_{ij}(t)$ between wells i and j, and the energy ϵ of the potential wells:

$$H_{3w} = \sum_{i=1}^{3} \epsilon c_i^\dagger c_i + (\hbar\Omega_{12}(t) c_1^\dagger c_2 + \hbar\Omega_{23}(t) c_2^\dagger c_3 + \text{H.c.}), \tag{1}$$

where $c_i^\dagger$ creates an electron in well i.

We now wish to apply the CTAP scheme to coherently transfer an electron from well 1 to well 3. Following Ref. [1], this is achieved by applying Gaussian voltage pulses to tune the tunnel barriers in time according to

$$\Omega_{12}(t) = \Omega_{\max} \exp\left[-\frac{(t - t_{\max}/2 - t_{\text{delay}})^2}{2\sigma^2} \right],$$
$$\Omega_{23}(t) = \Omega_{\max} \exp\left[-\frac{(t - t_{\max}/2)^2}{2\sigma^2} \right], \tag{2}$$

where we introduced the pulses height ($\Omega_{\max}$) and duration ($t_{\max}$), and chose for the standard deviation $\sigma = t_{\max}/8$. The pulses are applied in a counterintuitive sequence (Ω_{23} is fired prior to Ω_{12}) with a delay $t_{\text{delay}} = 2\sigma$, in order to maximize the fidelity of the transfer [1,14].

To monitor the charge configuration of this system, we couple the middle potential well to a charge detector. Here we use a simplified version of the QPC, namely, a tunnel junction whose barrier height is sensitive to the presence of an electron in the middle well. The hopping amplitude through the barrier varies from Ω' to Ω, depending on whether or not well 2 is occupied [15]. The detector Hamiltonian can thus be written as

$$H_{qpc} = \sum_r E_r a_r^\dagger a_r + \sum_l E_l a_l^\dagger a_l + \sum_{l,r} \hbar(\Omega + \delta\Omega c_2^\dagger c_2)(a_r^\dagger a_l + a_l^\dagger a_r), \tag{3}$$

where $a_r^\dagger$ and $a_l^\dagger$ are the electron creation operators in the right and left electrode, respectively, while $E_{r,l}$ stands for the set of energy levels in the reservoirs. Here we introduced $\delta\Omega = \Omega' - \Omega$, and assumed all tunneling amplitudes to be real and energy independent.

Our goal is to study the evolution of the triple-well system under continuous measurement by the detector, focusing on a single realization of the measurement process. This is achieved by considering the triple-well system and the detector as the two parts of an enlarged quantum system. This allows for describing the quantum state of this enlarged system via a generalized density matrix $\rho_{ij}^n(t)$ [15]. The latter corresponds to the density matrix in the basis of localized states (associated with wells 1, 2, and 3) further divided into components with different number n of electrons passed through the detector. The evolution of this generalized density matrix is given by a set of Bloch-type equations obtained from the many-body Schrödinger equation for the entire system. Extending the derivation of Ref. [15] to include time-dependent tunneling rates, one obtains the following set of rate equations for the density matrix

$$\begin{aligned}
\dot\rho_{11}^n(t) &= D[\rho_{11}^{n-1}(t) - \rho_{11}^n(t)] - 2\Omega_{12}(t)\text{Im}[\rho_{12}^n(t)],\\
\dot\rho_{22}^n(t) &= D'[\rho_{22}^{n-1}(t) - \rho_{22}^n(t)] + 2\Omega_{12}(t)\text{Im}[\rho_{12}^n(t)]\\
&\quad - 2\Omega_{23}(t)\text{Im}[\rho_{23}^n(t)],\\
\dot\rho_{33}^n(t) &= D[\rho_{33}^{n-1}(t) - \rho_{33}^n(t)] + 2\Omega_{23}(t)\text{Im}[\rho_{23}^n(t)],\\
\dot\rho_{12}^n(t) &= \sqrt{DD'}\rho_{12}^{n-1}(t) - \frac{D + D'}{2}\rho_{12}^n(t)\\
&\quad + i\Omega_{12}(t)[\rho_{11}^n(t) - \rho_{22}^n(t)] + i\Omega_{23}(t)\rho_{13}^n(t),\\
\dot\rho_{23}^n(t) &= \sqrt{DD'}\rho_{23}^{n-1}(t) - \frac{D + D'}{2}\rho_{23}^n(t)\\
&\quad + i\Omega_{23}(t)[\rho_{22}^n(t) - \rho_{33}^n(t)] - i\Omega_{12}(t)\rho_{13}^n(t),\\
\dot\rho_{13}^n(t) &= D[\rho_{13}^{n-1}(t) - \rho_{13}^n(t)] + i\Omega_{23}(t)\rho_{12}^n(t)\\
&\quad - i\Omega_{12}(t)\rho_{23}^n(t),
\end{aligned} \tag{4}$$

where we used the convention $\rho_{ij}^0(t) = 0$, and introduced the tunneling rates $D = 2\pi\hbar\rho_R\rho_L\Omega^2 eV$ and $D' = 2\pi\hbar\rho_R\rho_L\Omega'^2 eV$. Here, we considered a QPC under a voltage bias V, with constant density of states $\rho_{R,L}$ in the electrodes. Note that by tracing over the detector degrees of freedom, one recovers the conventional master equation for the density matrix $\rho_{ij} = \sum_n \rho_{ij}^n$. In this case, the measurement backaction reduces to a constant dephasing term $\Gamma = (\sqrt{D} - \sqrt{D'})^2/2$, which only affects the coherences ρ_{12} and ρ_{23}.

The drawback in including the detector into the quantum part of the setup is that one now needs a way to extract classical information from it. Following Ref. [13], we introduce a classical pointer which periodically collapses the wave function of the quantum system. The pointer only interacts with the detector at times t_k, forcing it to choose a definite value n_k for the number $n(t_k)$ of electrons that passed through the QPC. The value of n_k is picked randomly according to the probability distribution $P(n)$ set by the density matrix at the time of the collapse, namely $P(n) = \rho_{11}^n(t_k) + \rho_{22}^n(t_k) + \rho_{33}^n(t_k)$. Once a particular n_k has been selected, the density matrix should be immediately updated as $\rho_{ij}^n(t_k^+) = \delta_{n,n_k}\rho_{ij}^{n_k}(t_k^-)/P(n_k)$. After that, the system evolves according to Eq. (4) until the next collapse at $t = t_{k+1}$. While it is not clear how frequently the collapse procedure should occur, we could check explicitly that our results are insensitive to the choice of t_k, provided that $\Delta t_k = t_k - t_{k-1} \ll t_{\max}$.

The combination of the coupled Bloch Eqs. (4) with the collapse procedure is solved by stochastic sampling: for a given sequence of times t_k, we numerically implement the

succession of evolutions and collapses while keeping track of the detector output $n(t)$. This provides us with one particular realization of the measurement process. In particular, this implies that by the end of the "simulated experiment" at $t = \tau$, one obtains a definite answer whether the electron sits in the middle well or not, so that $\rho_{22}^{n(\tau)}(\tau)$ can only take the values 0 or 1. Moreover, reproducing this procedure over thousands of realizations allows us to extract statistical properties, such as the distribution $\mathcal{P}(n)$ of the total number of electrons that crossed the tunnel junction over the duration τ of the experiment. Such features could be compared to experimental data when it becomes available.

As a first test of the method, we consider the case of a decoupled detector, obtained by setting equal tunneling rates $D = D'$ in Eq. (4). In this case, no information on the position of the electron can be extracted from the measurement and the CTAP scheme works with optimum fidelity. We could verify not only that the distribution $\mathcal{P}(n)$ obtained after a few thousand runs turns out to be very close to the expected Poisson behavior but also that the profile of the diagonal density matrix $\rho_{ii}^{n_k}(t_k^+)$ is identical to the one obtained from solving the conventional master equation for $\rho_{ii}(t)$ with Hamiltonian H_{3w} (1).

Let us now increase the coupling to the detector, by reducing the value of the tunneling rate D' compared to D. Keeping track of the distribution $\mathcal{P}(n)$ of the number of electrons in the detector as a function of the rate mismatch $D - D'$ leads to the results of Fig. 1(a). The main signature of the measurement backaction on this distribution is the emergence of a satellite peak on top of the Poisson-like behavior. As one increases the value of $D - D'$, making the measurement stronger, this secondary structure becomes more prominent, while the main peak flattens out. The distance between these two features grows like $(D - D')\tau$. Out of the thousands of realizations that result in the distribution of Fig. 1(a), the ones that contribute to the satellite peak correspond to situations for which the electron sits in the middle well by the end of the experiment, i.e. $\rho_{22}^{n(\tau)}(\tau) = 1$. As a result, the integral under this secondary peak measures the proportion p_2 of runs where the electron is detected in well 2. Obviously, these realizations exemplify an unsuccessful transfer, and one would thus expect a reduced fidelity for the CTAP scheme. Indeed, as the coupling to the detector becomes more important, one obtains more information on the location of the electron, and the fidelity of the CTAP protocol decreases, as shown in Fig. 2(a). This reduction turns out to be more important than one would anticipate because the average probability p_1 of finding the electron in the first potential well is not only finite but also increases along with $D - D'$ in a way that $p_1 \simeq p_2$; see Fig. 2(a). The measurement therefore leads to an increased population of the middle well, compared to the unmonitored CTAP scheme. This effect is quantitatively similar to that of pure dephasing [1].

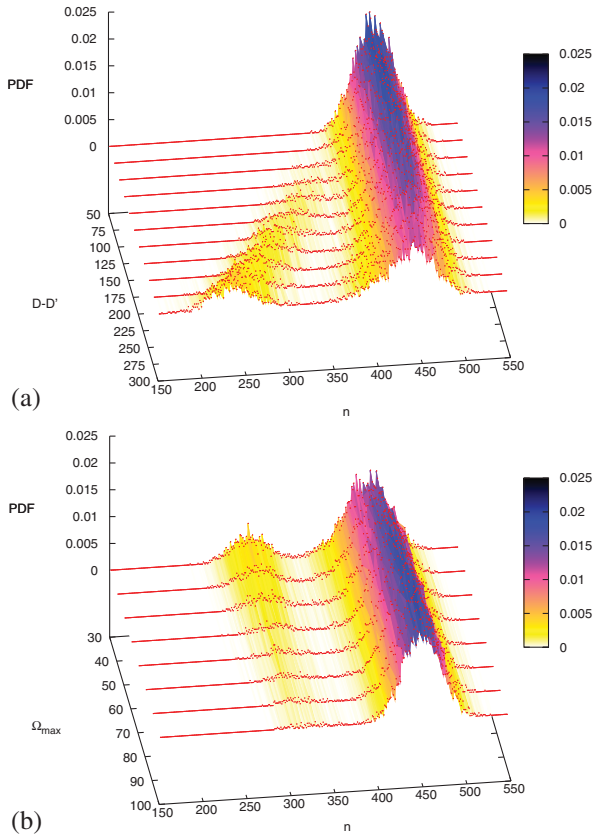

FIG. 1 (color). Distribution $\mathcal{P}(n)$ as a function of (a) $D - D'$ with $\Omega_{\max} = 50$, $D = 300$ (in units of $t_{\max}^{-1}$), (b) $\Omega_{\max}$, for $D = 300$, $D' = 100$ (in units of $t_{\max}^{-1}$). In both cases, the duration of the experiment is $\tau = 1.5t_{\max}$.

We could further check that for a given value of $D - D'$ increasing the amplitude $\Omega_{\max}$ of the pulses restores the fidelity of the CTAP protocol, as illustrated in Fig. 2(b). This, however, goes with a significant loss of weight of the satellite peak in the probability distribution $\mathcal{P}(n)$ [see Fig. 1(b)] corresponding to a loss of information on the location of the electron. These results also confirm that the position of the satellite peak is independent of $\Omega_{\max}$.

The compiled record of the detector output $n(t)$ for 1000 runs is plotted in Fig. 3, and one readily sees that it can be divided into two subsets. The lower subset is associated with the ensemble of runs that contribute to the satellite peak in $\mathcal{P}(n)$, and correspond to the detection of the electron in the middle well, $\rho_{22}^{n(\tau)}(\tau) = 1$. The upper subset is associated with the ensemble of runs contributing to the main Poisson-like structure in $\mathcal{P}(n)$, and correspond to $\rho_{22}^{n(\tau)}(\tau) = 0$.

It is instructive to evaluate the average behavior of $n(t)$ within each of these subsets (see inset of Fig. 3). On average, for the upper subset one has $\langle n(t)\rangle \sim Dt$, with a very small downward shift compared to the straight line. For the lower subset, there are three distinct regimes, defined by the typical scales $t_{\max}$ and t_{cross} [defined as $\Omega_{12}(t_{\text{cross}}) = \Omega_{23}(t_{\text{cross}})$]. For $0 \leq t \lesssim t_{\text{cross}}$, the average number $\langle n(t)\rangle$ of electrons through the detector is again

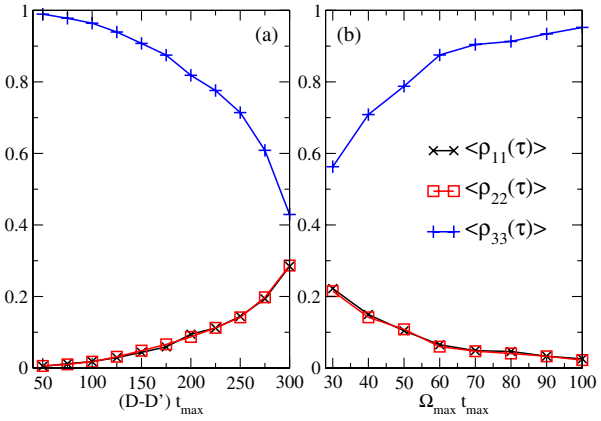

FIG. 2 (color online). Diagonal part of the density matrix $\rho_{ii}^{n(\tau)}(\tau)$ averaged over all runs, as a function of (a) $D - D'$ with $\Omega_{\max} = 50$, $D = 300$ (in units of $t_{\max}^{-1}$), (b) $\Omega_{\max}$, for $D = 300$, $D' = 100$ (in units of $t_{\max}^{-1}$). In both cases, the duration of the experiment is $\tau = 1.5t_{\max}$.

given by Dt and the average occupation of the middle well stays much lower than 1. For times $t \gtrsim t_{\max}$, $\langle n(t)\rangle$ grows like $D't$ and the average occupation of the middle well stays close to 1, over the whole time range: the electron has been detected. The most interesting behavior occurs for $t_{\text{cross}} \lesssim t \lesssim t_{\max}$: the detection builds up as the average occupation of the middle well rises from nearly 0 to nearly 1. In the meantime, the average detector output $\langle n(t)\rangle$ grows like $(D + D')t/2$, while one might have expected a gradual decrease of the slope from D to D'. This slope is a robust feature which does not seem to depend on the ratio t_{delay}/σ, or the Gaussian nature of the pulses (2). For convenience, we chose to present results obtained for a substantial value of $D - D'$, as it enhances the features observed. We could verify however, that much smaller values of this parameter (e.g., $D - D' = 0.1$ D) lead to very similar results, and, in particular, one can still isolate three regimes in the detector output with the same

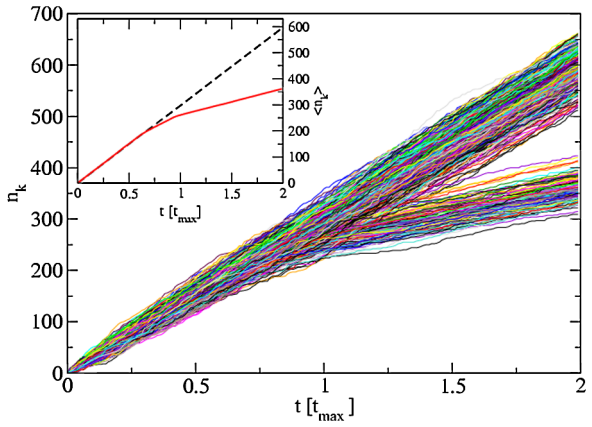

FIG. 3 (color online). Compiled (main graph) and averaged (inset) record for the upper and lower subsets, obtained for 1000 runs, with $\Omega_{\max} = 50$, $D = 300$, $D' = 100$ (in units of $t_{\max}^{-1}$) and a duration of the experiment $\tau = 2t_{\max}$.

intriguing slope in the intermediate one. Finally, notice that it is fundamentally impossible to derive measurement records like the ones shown in Fig. 3 from a conventional master equation description [1].

Our approach can easily be extended to other pulse shapes and sequences as well as more complicated setups. It also offers the possibility to reconstruct the density matrix for a given experiment, by replacing the random collapse with the experimental measurement record.

In summary, we have proposed an approach which allows to study the measurement backaction on an electron submitted to the CTAP protocol in a triple-well system. Our work captures the loss of fidelity of the CTAP scheme associated with the measurement process, a feature generally accounted for in the conventional master equation formalism by explicitly adding a dephasing term. The key observation of this Letter is that the reduction of the fidelity is directly connected to the amount of information one can extract concerning the location of the electron. This has the important implication that a decohering environment coupling to an electron on the CTAP chain reduces the fidelity of this scheme for quantum information transfer in spite of the fact that the occupation probability along the chain can be made arbitrarily small for the case without decoherence.

We are grateful to J. H. Cole, A. Korotkov and S. Ludwig for helpful discussions. This work was supported through SFB 631 of the Deutsche Forschungsgemeinschaft, the Center for NanoScience (CeNS) Munich, and the German Excellence Initiative via the Nanosystems Initiative Munich (NIM).

[1] A. D. Greentree *et al.*, Phys. Rev. B **70**, 235317 (2004).
[2] N. V. Vitanov *et al.*, Annu. Rev. Phys. Chem. **52**, 763 (2001).
[3] D. Schörer *et al.*, Phys. Rev. B **76**, 075306 (2007).
[4] D. Petrosyan and P. Lambropoulos, Opt. Commun. **264**, 419 (2006).
[5] J. H. Cole *et al.*, Phys. Rev. B **77**, 235418 (2008).
[6] T. Opatrny and K. K. Das, Phys. Rev. A **79**, 012113 (2009).
[7] R. Rahman *et al.*, Phys. Rev. B **80**, 035302 (2009).
[8] J. Siewert, T. Brandes, and G. Falci, Opt. Commun. **264**, 435 (2006).
[9] K. Eckert *et al.*, Phys. Rev. A **70**, 023606 (2004); K. Eckert *et al.*, Opt. Commun. **264**, 264 (2006).
[10] E. M. Graefe, H. J. Korsch, and D. Witthaut, Phys. Rev. A **73**, 013617 (2006); M. Rab *et al.*, Phys. Rev. A **77**, 061602 (R) (2008).
[11] S. Longhi *et al.*, Phys. Rev. B **76**, 201101 (2007).
[12] I. Kamleitner, J. Cresser, and J. Twamley, Phys. Rev. A **77**, 032331 (2008).
[13] A. N. Korotkov, Phys. Rev. B **63**, 115403 (2001); A. N. Korotkov, in *Quantum Noise in Mesoscopic Physics*, edited by Yu. V. Nazarov (Kluwer, Netherlands, 2003), p. 205.
[14] U. Gaubatz *et al.*, J. Chem. Phys. **92**, 5363 (1990).
[15] S. A. Gurvitz, Phys. Rev. B **56**, 15215 (1997).